Post-print of: Hejna A., Kirpluks M., Kosmela P., Cabulis U., Haponiuk J., Piszczyk Ł.: The influence of crude glycerol and castor oil-based polyol on the structure and performance of rigid polyurethane-polyisocyanurate foams. INDUSTRIAL CROPS AND PRODUCTS. Vol. 95, (2017), p. 113-125. DOI: 10.1016/j.indcrop.2016.10.023

The influence of crude glycerol and castor oil-based polyol on the structure and performance of rigid polyurethane-polyisocyanurate foams

Aleksander Hejna [a], Mikelis Kirpluks [b], Paulina Kosmela [a], Ugis Cabulis [b], Józef Haponiuk [a], Łukasz Piszczyk [a]

[a] Department of Polymer Technology, Chemical Faculty, Gdansk University of Technology, G. Narutowicza Str. 11/12, G. 80-233 Gdansk, Poland
[b] Latvian State Institute of Wood Chemistry, 27 Dzerbenes, LV 1006 Riga, Latvia

a b s t r a c t

In this work, biopolyol obtained from two types of industrial crops' processing products: crude glycerol and castor oil was used for preparation or rigid polyurethane-polyisocyanurate foams. Bio-based polyol was obtained via crude glycerol polymerization and further condensation of resulting polyglycerol with castor oil. Rigid polyurethane-polyisocyanurate foams were prepared at partial substitution (0–70 wt.%) of petrochemical polyol with synthesized bio-based polyol. Influence of the biopolyol content on the chemical and cellular structure, insulation properties, static and dynamic mechanical properties, ther-mal degradation and fire behavior of foams was investigated. Incorporation of crude glycerol-based polyol into formulation of rigid polyurethane-polyisocyanurate foams had beneficial impact on the structure of material reducing average cell size from 372 to 275 μm and increasing closed cell content from 94.0 to 95.7%. Such changes resulted in 7% decrease of thermal conductivity coefficient to 21.8 mW/(m K). Mechanical performance of foams was enhanced by partial substitution of petrochemical polyol with synthesized biopolyol. Compressive strength of modified foam was more than 90% higher than for refer-ence sample. The modifications of foams caused changes in thermal degradation pathway, nevertheless thermal stability of the reference foam was maintained. Incorporation of crude glycerol-based polyol into foams' formulation decreased maximum value of heat release rate by 3.5%, increased char residue after combustion by 24% and reduced emission of toxic carbon monoxide during burning of foam by 35%.

Keywords: Bio-based polyols, Crude glycerol, Castor oil, Rigid polyurethane-polyisocyanurate foams, Cellular structure, Thermal properties

1. Introduction

Various legislation regulations, such as European Union directives or Provisions of the Kyoto Protocol intend to reduce the greenhouse gases emission (Hoekman et al., 2012). Quite simple and obvious way to inhibit the excessive emission of CO_2 is the use of energy and raw materials from renewable resources. Nowadays, polyurethane (PU) industry is strongly depending on the petroleum, since majority of components used in PU manufacturing is petroleum-based (Allauddin et al., 2016). Nevertheless, petroleum is non-renewable raw material, whose availability will be limited and price will be growing in the future. Having this in mind, researchers became focused on environmentally friendly efforts, and intensive development of technologies based on ecological materials has started (Arshanitsa et al., 2016; Kairyte and Vejelis, 2015; Tong et al., 2015). Various sources have been investigated as raw materials for biopolyols production, mainly vegetable oils, such as rapeseed, sunflower, palm, coconut, linseed or soybean oils (Amir Uddin and Azad, 2012; Kurańska and Prociak, 2016; Kurańska et al., 2016; Scholz and da Silva, 2008; Zieleniewska et al., 2015). However, these oils are successfully used in food industry and their broader incorporation into PU industry might have unfavorable influence on the price of different food products. That is why scientific and industrial circles have been lately focused on the application (in PU manufacturing) of various by-products from processing of crops and other renewable materials, like the most popular crude glycerol originated from production of biodiesel, which generally is a product of industrial processing of rapeseed oil.

http://dx.doi.org/10.1016/j.indcrop.2016.10.023

For each ton of produced biodiesel, around 100 kg of glycerol is obtained (Choi, 2008). Estimating current European production of biodiesel as exceeding 9.5 million tonnes, almost 1 million tonnes of crude glycerol is generated annually in Europe (Puri et al., 2012; Ragauskas et al., 2006). Such glycerol, however, contains various impurities – water, soaps, fatty acids and their esters, methanol and catalyst of transesterification, mainly KOH (Thompson and He, 2006). Detailed composition of crude glycerol depends on the type of used raw materials, applied catalyst and post-reaction processes, such as acidification or demethylation. Incorporation of crude glycerol into PU industry does not require complicated and often expensive purification processes, in contrary to the utilization of glycerol in food, pharmaceutical or cosmetics industry (Yazdani and Gonzalez, 2007). Crude glycerol can be applied in PU manufacturing in various ways, which can be divided into two groups: direct and indirect. Indirect approaches include use of compounds obtained from crude glycerol, such as propanediol and butanediol resulting from microbial conversion (Petrov and Petrova, 2010; Szymanowska-Powałowska, 2014) or glycerol carbonate from glycerol carboxylation or glycerolysis of urea (Casiello et al., 2014; Ezhova et al., 2012; Jagadeeswaraiah et al., 2014; Nguyen and Demirel, 2013). Direct methods include using of biopolyols produced through lignocellulose biomass liquefaction (Cheng et al., 2014; Hu and Li, 2014; Hu et al., 2012) or by polymerization of crude glycerol (Nik Siti et al., 2013). Obviously, simpler and economically more beneficial are direct approaches.

Polymerization process of glycerol can be performed using different types of catalysts (preferably base catalysts) and resulting polyglycerol may be successfully used in preparation of polymeric materials (Salehpour and Dubé, 2012). Various complicated catalysts have been used in glycerol polymerization, such as zeolites (Melero et al., 2012), mesoporous materials (Clacens et al., 2000) or ion-exchange resins (Klepáčová et al., 2005), however the most popular are the simpler ones, metal hydroxides (Salehpour and Dubé, 2011). Microwave irradiation was also applied at polymerization of crude glycerol in order to eliminate the use of catalysts (Nik Siti et al., 2013). Also conditions of the process have noticeable effect on final properties of polyglycerols. Lower reaction temperatures and low pH values result in the formation of cyclic isomers, while at elevated temperatures side reactions show unfavorable influence on color and smell of final products.

Polyglycerols, because of their branched structure can be considered as very interesting substrates for synthesis of highly cross-linked PU materials, such as rigid PU foams (Li et al., 2014).

Ionescu and Petrovic (2010) synthesized polyether polyols based on polyglycerol. First step of the process was polycondensation of pure glycerol in the presence of potassium methoxide or potassium hydroxide. Later, polyglycerols were subjected to propoxylation in order to prepare high functionality polyether polyols. Resulting biopolyols were used in manufacturing of rigid PU foams, which showed good physical and mechanical properties, especially very good dimensional stability and low friability.

Luo et al. (2013) analyzed the influence of process parameters (time and temperature of reaction) and the content of catalyst (sulfuric acid) on the properties of biopolyols produced from crude glycerol. Polyol prepared under preferential conditions (200 °C, 90 min, 3 wt.% of sulfuric acid) was characterized by hydroxyl value of around 480 mg KOH/g, acid number lower than 5 mg KOH/g and viscosity about 25 Pa s. Subsequently, authors used obtained biopolyols to prepare PU foams, which showed comparable properties to petroleum-based materials – apparent density of 43 kg/m^3 and compressive strength of 185 kPa.

In previous work (Piszczyk et al., 2014b) we used two types of commercially available polyglycerols from Eco Innova, named Pole and PGK. Substitution of 35 and 70 wt.% of commercial Rokopol RF551 by polyglycerols resulted in the increase of apparent density and simultaneous enhancement of mechanical performance of polyurethane foams. Moreover, incorporation of 35 wt.% of polyglycerols did not affect the cellular structure and thermal properties of foams, hardly any changes in cell size, closed cell content and thermal conductivity coefficient were observed.

Table 1
Properties of polyols used for the production of rigid polyurethane-polyisocyanurate foams.

Property	Polyol		
	CG	Lupranol 3300	Lupranol 3422
Density, g/cm^3	1.18	1.05	1.09
Hydroxyl number, mg KOH/g	460	400	490
Viscosity, mPa s	840	373	22750
Water content, wt.%	0.207	0.368	0.301

Majority of the research works focused on the incorporation of bio-based polyols into PU foams. Nevertheless, it seems more interesting to develop formulations for rigid polyurethane-polyisocyanurate (PU-PIR) foams, which are nowadays substituting conventional PU foams, due to their superior thermal properties and fire resistance. Manufacturing of PU-PIR foams requires adjustment of recipe comparing to unmodified polyurethane foams, therefore proper examination of crude glycerol-based polyols is required.

In this work the potential of biopolyol prepared from industrial crops' processing products: crude glycerol (by-product from production of biodiesel, prepared from rapeseed or soybean) and castor oil (obtained from ricinus) in the manufacturing of rigid PU-PIR foams is evaluated. In the light of above mentioned studies, we aimed to examine the possibility of partial substitution of petrochemical based polyol with biopolyol and the influence of its share in polyol mixture (0–70 wt.%) on the chemical (FTIR studies) and cellular (SEM analysis, determination of closed cell content) structure, mechanical (compression tests, dynamic mechanical analysis) and thermal (thermogravimetric analysis, thermal conductivity coefficient measurement) properties and fire behavior of resulting rigid foams.

2. Experimental

2.1. Materials

Bio-based polyol was synthesized from crude glycerol and castor oil. Crude glycerol was acquired from Bio-Chem Sp. z o.o. (Poland), while castor oil was acquired from Pro-Lab (Poland). 85% aqueous solution of ortophosphoric acid was used as a catalyst and 50% aqueous solution of sulfuric (VI) acid was used to neutralize reaction products. Both acids were obtained from POCH S.A. (Poland).

Rigid PU-PIR foams were prepared from previously obtained bio-based polyol, later noted as CG (like crude glycerol) and commercially available polyols from BASF company, Lupranol 3300 (trifunctional polyether based on glycerol) and Lupranol 3422 (high functional polyether based on sorbitol). Two different petrochemical polyols were applied in order to exploit their advantages – low viscosity, hence easier processability of Lupranol 3300 and higher functionality of Lupranol 3422 resulting in enhancement of foams' crosslink density (Andersons et al., 2015; Kirpluks et al., 2014). Basing on the viscosity of CG biopolyol it was used as a substitute of Lupranol 3300 in combination with high-functionality Lupranol 3422. The properties of the aforementioned polyols are presented in Table 1.

Isocyanate used in the reaction was polymeric 4,4′-methylene diphenyl diisocyanate (pMDI) characterized by a 31.5% content of NCO groups (BASF). The average functionality of pMDI was c.a. 2.8.

Table 2
Changes in hydroxyl value during polymerization of crude glycerol.

Time, min	0	60	120	180	240	300	360
Hydroxyl value, mg KOH/g	640	648	661	664	605	582	523

Tris(1-chloro-2-propyl)phosphate (TCPP) produced by LANXESS Deutschland GmbH (Levagard PP – technical name) was used as flame retardant. Potassium acetate (PC CAT® TKA30) and tertiary amine (PC CAT® NP-10) produced by Performance Chemicals were used as catalysts. Niax Silicone (L-6915) produced by Momentive Performance Materials Inc. was used as a stabilizer of porous structure. Distilled water and liquid hydrofluorocarbon blend (Solkane® 365/227) were used as a chemical and physical foaming agent, respectively.

2.2. Synthesis of bio-based polyol

As mentioned before bio-based polyol was synthesized from crude glycerol and castor oil according to patent application developed at the Department of Polymer Technology of Gdańsk University of Technology (Piszczyk et al., 2014a). Crude glycerol used in this study was characterized by hydroxyl value of 525 ± 28 mg KOH/g and acid number of 1.92 mg KOH/g. Chosen parameters of the reaction were based on literature studies of previous works (Miyata et al., 2012; Wirpsza and Banasiak, 2012). First step was polymerization of crude glycerol, which was carried out in 1L reactor equipped with mechanical stirrer. According to literature data 3 wt.% of catalyst was added, which should provide appropriate conditions for the polymerization (Wirpsza and Banasiak, 2012). The reaction was carried out in vacuum at 180 °C for 6 h. Samples were collected first after reaching desired temperature and then every 60 min in order to control the hydroxyl value of resulting polyol. Results are presented in Table 2.

As mentioned before, initial hydroxyl value of applied crude glycerol was 525 mg KOH/g. Higher hydroxyl values at start of the reaction (reaction time of 0 h) are related to the addition of catalyst – potassium hydroxide, which was added as saturated aqueous solution, in order to introduce as little water as possible into the system. Increase of hydroxyl value at early stages of reaction is related to presence of water, which was generated as a by-product of glycerol polycondensation. In Fig. 1 there is presented general scheme of glycerol condensation and in Fig. 2 possible structures of obtained polyglycerol were provided. Generally, polyglycerols obtained by condensation of glycerol in presence of basic catalysts are high functionality mixture of linear, branched and cyclic structures of different polycondensation degrees (Kainthan et al., 2006). Content of linear polyglycerols is the highest, followed by branched structures. Cyclic structures stand for less than 10% of total amount of obtained polyglycerol (Cassel et al., 2001).

Next step was condensation of resulting polyglycerol with castor oil in order to decrease the viscosity and hydroxyl value of final product. Moreover, neat polyglycerols are considered to be incompatible with aromatic isocyanates, such as pMDI used in this study (Ionescu and Petrovic, 2010). Castor oil was chosen because of the high content of ricinoleic acid, which has in its structure both carboxyl and hydroxyl group (in Fig. 3 there are shown chemical structures of three main fatty acid components of castor oil). When combined with polyglycerol it is decreasing the hydroxyl value of polyol, through reduction of hydroxyl groups' density, without the reduction of polyol functionality.

Previously prepared polyglycerol and castor oil were mixed, 50% excess of castor oil was used (castor oil: polyglycerol ratio 1.5:1), in the presence of 7.5 g of ortophosphoric acid. Synthesis was carried on at 180 °C for 5 h, basing on the literature data (Zhang et al., 2014). Scheme of reaction and proposed structure of obtained biopolyol are presented in Fig. 4. Ricinoleic acid is able to link with polyglycerol through both carboxyl and hydroxyl groups, nevertheless the reaction is considered as transesterification, so bonding through carboxyl group and generation of ester bond is more probable. Resulting polyol was characterized by hydroxyl value of 460 mg KOH/g of resin and pH value of 9.7. Last step was the neutralization of polyol to pH equaling 7 using sulfuric acid.

2.3. Polyurethane foam preparation

Rigid PU-PIR foams were produced on a laboratory scale by a single step method from a two-component (A and B) system with the isocyanate index (which is the ratio of the equivalent amount of isocyanate used relative to the theoretical equivalent amount times 100) equal to 200.

The component A (polyol mixture), consisting of the appropriate amounts of Lupranol 3422, bio-based polyol CG or their mixtures with oligoether Lupranol 3300 at various ratios, flame retardant, catalysts, surfactant and foaming agents, was weighed and placed in a 500 ml polystyrene cup. Next, the polyol mixture was homogenized with a mechanical stirrer at 2000 rpm for 20 s. Such prepared component A was mixed with component B (pMDI) at a predetermined mass ratio and stirred at 2000 rpm for 20 s. The resulting reaction mixture was poured into an open mold of dimensions 100 × 100 × 50 mm. Foams were cured for 24 h before demolding. After demolding, obtained samples were kept at 60 °C for 24 h and then conditioned at room temperature for 24 h. Table 3 contains the details of foam formulations.

2.4. Characterization

Hydroxyl value of bio-based polyol was determined according to PN-93/C-89052/03. Samples of 0.5 g were placed in 250 cm^3 Erlenmeyer flasks with acetylating mixture. Next, it was heated for 30 min, then 1 ml of pyridine and 50 ml of distilled water were added. Finally, resulting mixture was titrated using 0.5 M KOH solution in presence of phenolphthalein until the color of mixture changed to pink. Hydroxyl values were determined according to Formula (1):

$$HV = \frac{56,1 \cdot (V^2_{KOH} - V^1_{KOH}) \cdot C_{KOH}}{m} \quad (1)$$

where: C_{KOH} – concentration of KOH, $V^1{}_{KOH}$ and $V^2{}_{KOH}$ – volume of KOH used to titration of analyzed sample and blind test, m – mass of sample.

Viscosity of bio-based polyol was measured using R/S Portable rheometer. Shear rates of 1–100 s^{-1} were used, temperature of measurement was 25 °C.

FT-IR spectrophotometric analysis was performed in order to determine the structure of the bio-based polyol and rigid PU-PIR foams. The analysis was performed at a resolution of 4 cm^{-1} using a Nicolet 8700 apparatus (Thermo Electron Corporation) equipped with a snap-Gold State II which allows for making measurements in the reflection configuration mode.

After curing, foams were cut into samples whose properties were later determined in accordance with the standard procedures.

The apparent density of samples was calculated in accordance with EN ISO 845: 2000, as a ratio of the sample weight to the sample volume (g/cm^3). The cylindrical samples were measured with a slide caliper with an accuracy of 0.1 mm and weighed using electronic analytical balance with an accuracy of 0.0001 g.

The compressive strength of rigid foams was estimated in accordance with EN ISO 844:2007. The cylindrical samples with dimensions of 20 × 20 mm (height and diameter) were measured with a slide caliper with an accuracy of 0.1 mm. The compression

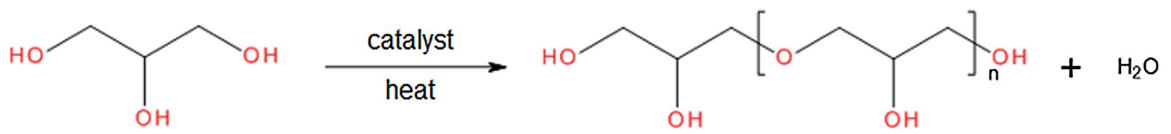

Fig. 1. General scheme of glycerol condensation resulting in polyglycerol.

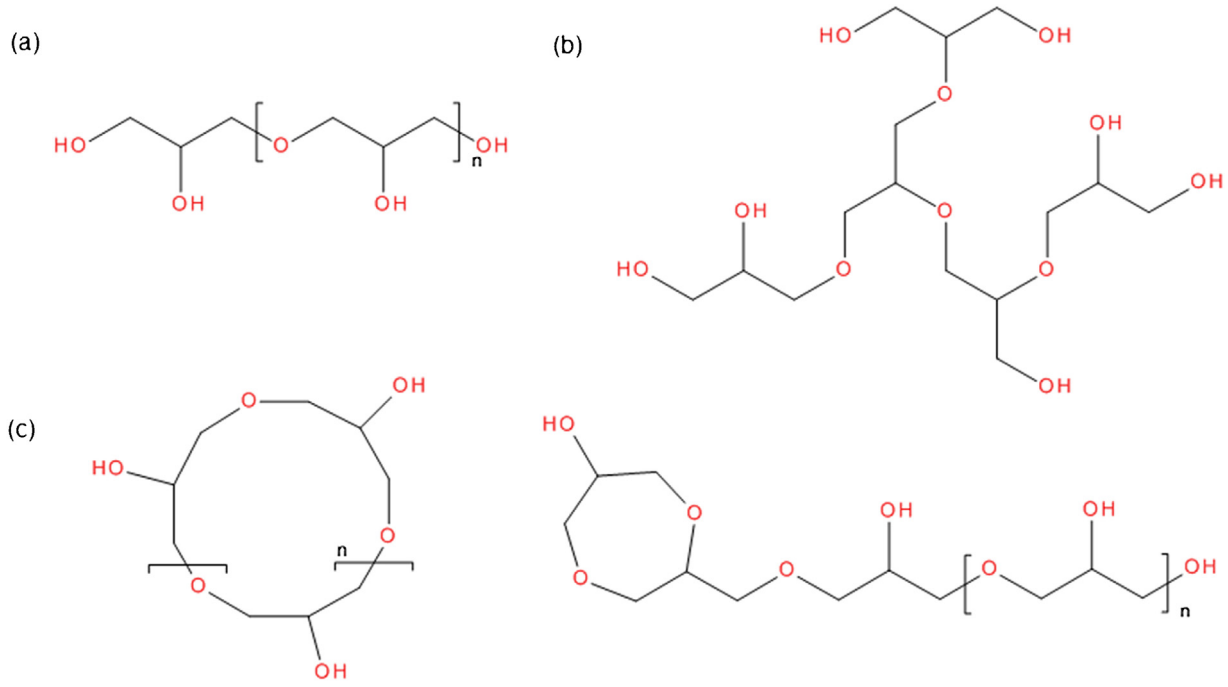

Fig. 2. Possible structures of obtained polyglycerol: (a) linear, (b) branched, (c) cyclic.

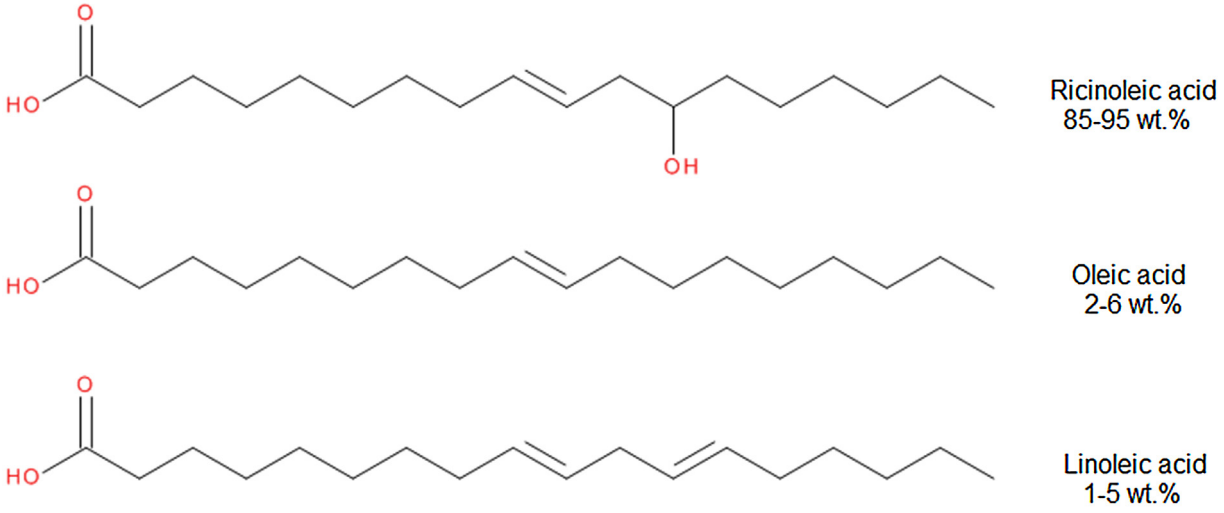

Fig. 3. Three main fatty acid components and their content in castor oil.

test was performed on a Zwick/Roell 1000 N testing machine at a constant speed of 10%/min until reaching 15% deformation.

A Tescan TS 5136 MM scanning electron microscope (SEM) with a secondary electron (SE) detector was used to take images of surface morphology. Before the SEM investigation, samples with a size of 1 × 1 × 0.2 cm were cut and sputtered with a gold layer using an Emitech K550X sputter coater (current 25 mA, coating time 2 min). Obtained data and images were processed with Vega TC software.

Closed cell content of prepared rigid PU-PIR foams was determined according to ISO 4590:2003.

Dynamic mechanical analysis was performed using DMA Q800 TA Instruments apparatus. Samples were analyzed in compression mode with a frequency of 1 Hz. Measurements were performed for the temperature range from 25 to 270 °C with heating rate 4 °C/min. Samples were cylindrical-shaped with dimensions of 8 × 12 mm.

The thermal conductivity in the range between 0 and 20 °C was tested with Linseis HFM (Heat Flow Meter) 200.

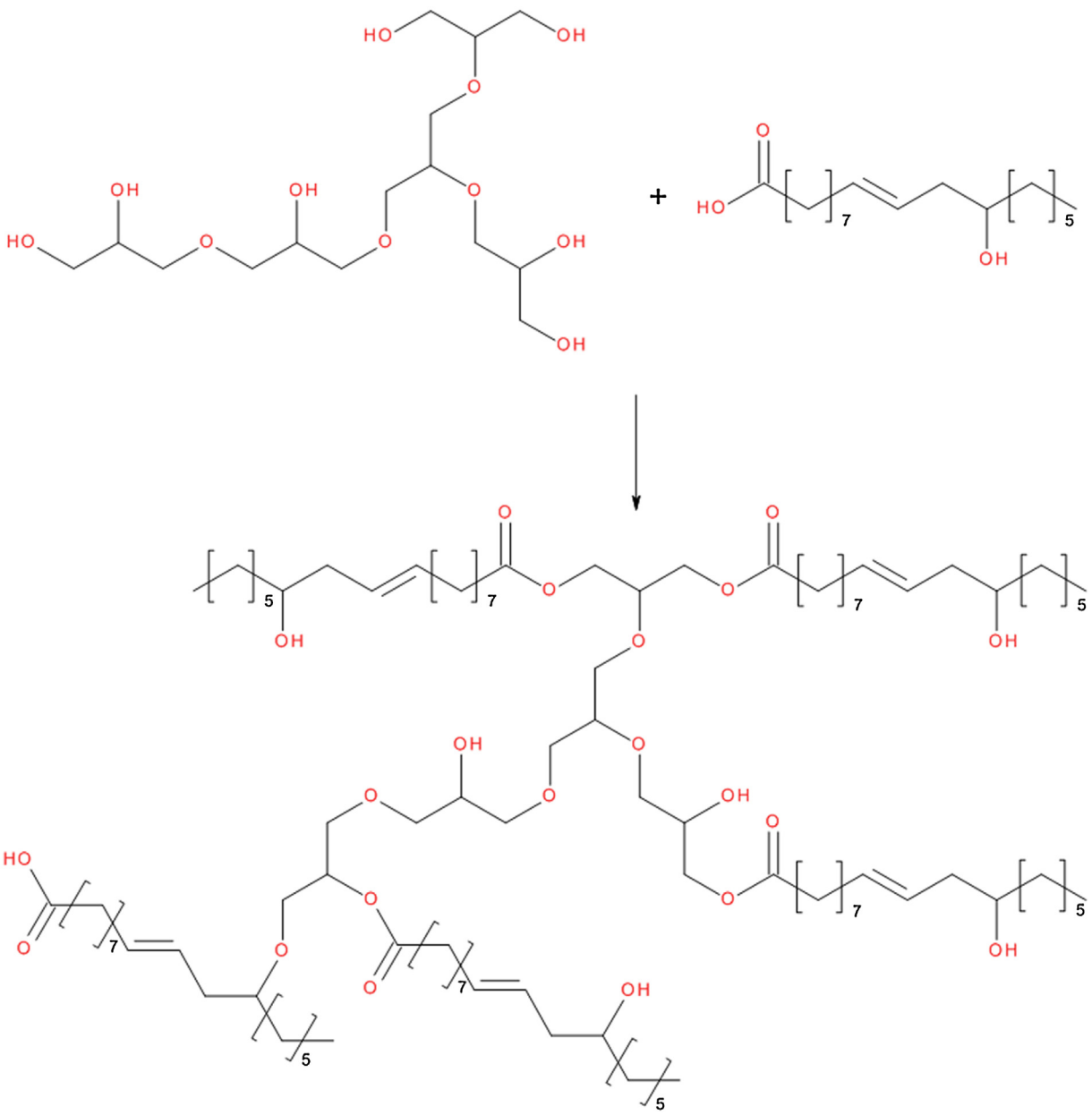

Fig. 4. General scheme of polyglycerol reaction with castor oil fatty acids.

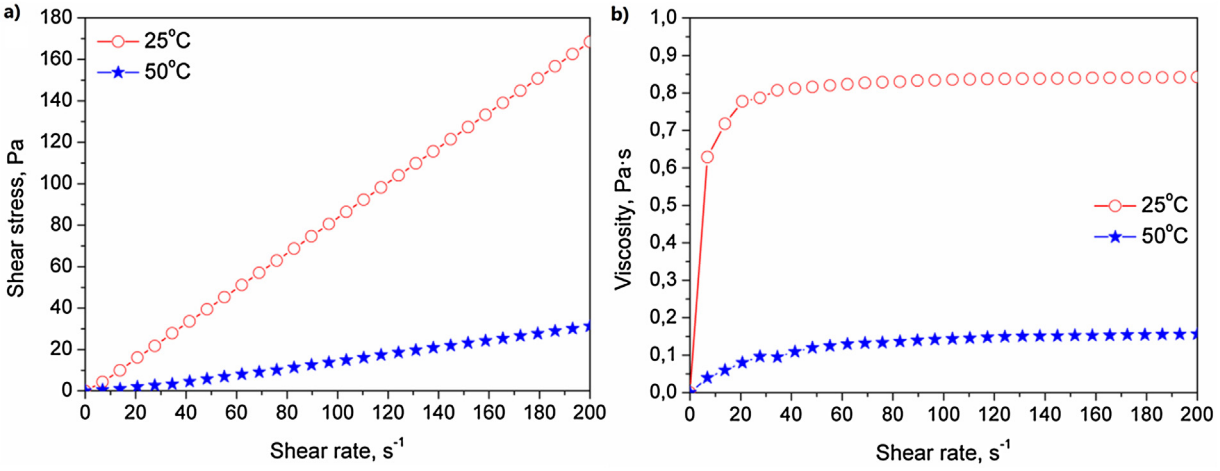

Fig. 5. Plots of shear stress (a) and viscosity (b) versus shear rate for bio-based polyol CG.

Table 3
Formulations of prepared PU-PIR foams.

Raw materials, pbw	Foam symbol				
	0CG	17.5CG	35CG	52.5CG	70CG
Lupranol 3422	30.0	30.0	30.0	30.0	30.0
Lupranol 3300	70.0	52.5	35.0	17.5	–
GC	–	17.5	35.0	52.5	70
TCPP	25.0	25.0	25.0	25.0	25.0
CAT NP-10	1.5	1.5	1.5	1.5	1.5
CAT TKA30	1.5	1.5	1.5	1.5	1.5
L-6915	2.0	2.0	2.0	2.0	2.0
Solkane	38.0	32.0	25.0	22.0	19.0
Water	0.5	0.5	0.5	0.5	0.5
Isocyanate	228.0	232.2	236.3	240.4	244.5
Isocyanate index	200	200	200	200	200
Content of bio-polyol in polyol mixture, wt.%	0	17.5	35.0	52.5	70.0
Content of bio-polyol in foam, wt.%	0	4.4	8.9	13.4	17.8

In order to evaluate the thermal stability of materials, thermogravimetric analysis (TGA) was performed on 5-mg samples by means of a NETZSCH TG 209 apparatus under argon atmosphere in the temperature range from 100 to 600 °C and at a heating rate of 20 °C/min.

The behavior of rigid PU-PIR foams under heat flux of 35 kW/m^2 during 300 s was tested using FTT Dual Cone Calorimeter. Tests were done according to ISO5660-1 standard. The following testing parameters were chosen: surface area – 88.4 cm^2; separation – 25 mm, orientation – horizontal. During the experiments, time required to initiate the reaction of combustion and thermo-kinetic parameters i.e. average heat release rate (HRR), total heat release (THR), total smoke released (TSR) were measured.

3. Results and discussion

3.1. Properties of CG bio-based polyol

In Fig. 5a there are presented flow curves of biopolyol CG plotted for 25 and 50 °C. Presented data indicate the non-Newtonian character of biopolyol, because of the nonlinear dependence of shear rate on shear stress (Chhabra, 2010; Dziubiński et al., 2009). Slope of the flow curves slightly increased with the increasing temperature, meaning that viscosity of prepared biopolyol is rising with temperature. Such behavior is typical for dilatant liquids. Fig. 5b showing plot of viscosity as a function of shear rate confirms observations made above. It can be seen that at low shear rate viscosity is increasing, while a higher shear rate values it is stabilizing, which points to dilatant character of obtained biopolyol (Singh and Heldman, 2013). Biopolyol CG shows value of viscosity in the same range as polyols used in manufacturing of rigid PU-PIR foams (see Table 1).

In Fig. 6 there are presented FTIR spectra of prepared biopolyol. A signal, which can be attributed to stretching vibrations of O—H groups was noticed at 3360 cm^{-1} (Deng and Ting, 2005). Peak at 3010 cm^{-1} was ascribed to the presence of C=C bonds in polyol structure. The absorption bands at 2850 and 2930 cm^{-1} can be associated with the symmetric and asymmetric stretching vibrations of C—H bonds in methylene groups present in aliphatic chains and methyl end groups. The signals at 1650 and 1730, could be attributed to the stretching vibrations of C=O bonds and unconjugated C=C stretching bonds in castor oil structure (Budarin et al., 2010). The absorption bands characteristic for CH_2 and C—OH in-plane bending vibrations were observed at 1380 and 1460 cm^{-1}. In the range of 1050–1170 cm^{-1} there can be observed multiplet absorption bands characteristic for vibrations of C—O—C ether and ester groups, which is related to the structure of prepared polyol. Polyglycerol part is considered to show polyether structure, however addition of fatty acids from castor oil definitely resulted in

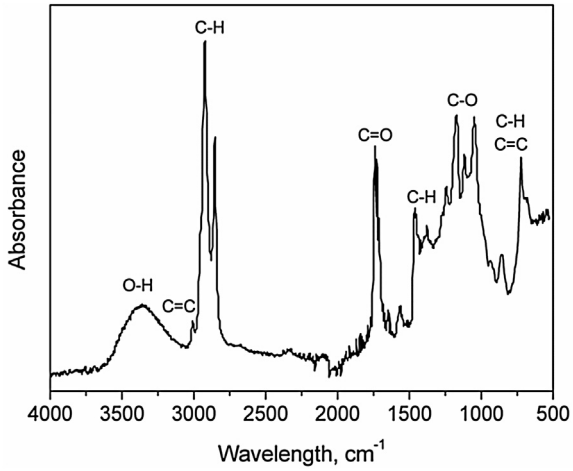

Fig. 6. FTIR spectra of prepared bio-based polyol CG.

creation of ester bonds (Cai et al., 2007). Other signals observed at 720, 860 and 930 cm^{-1} can be attributed to the out of plane vibrations of C=C and C—H bonds in methylene groups present in the structure of prepared material.

3.2. Properties of rigid PU-PIR foams

In Table 4 there are presented properties describing foams' cellular structure. As it can be seen all foams were characterized by almost the same value of apparent density. Formulations were specially developed (varying amount of Solkane 365/227) in order to provide the same density for all investigated materials, since apparent density is crucial parameter influencing performance of rigid PU-PIR foams. It can be seen (Table 3) that incorporation of crude glycerol-based polyol into foam decreased the amount of hydrofluorocarbon foaming agent necessary to provide the same density, even by 50%, which can be very beneficial from the economic and technological point of view.

In Table 4 there are presented average cell diameters of prepared rigid PU-PIR foams. Substitution of petrochemical polyol with biopolyol, up to 52.5 wt.% (content of CG in polyol mixture), resulted in noticeable decrease of cell size, which can be also seen on SEM images presented in Fig. 7. Considering values of standard deviation there are no significant differences between cell diameters of foams containing CG polyol. Nevertheless, it can be seen that partial substitution of Lupranol 3300 with biopolyol was beneficial for the cellular structure of rigid foams, which was also later confirmed by the measurements of closed cell content, thermal conductivity coefficient and compressive strength.Cell shape descriptors (cell

Table 4
Comparison of foams' properties.

Properties	Foam symbol				
	0CG	17.5CG	35CG	52.5CG	70CG
Apparent density, kg/m^3	47.3 ± 1.6	47.3 ± 1.4	47.1 ± 0.9	46.5 ± 1.4	46.5 ± 1.6
Average cell diameter, μm	372 ± 27	298 ± 35	283 ± 24	275 ± 21	276 ± 35
Cell aspect ratio	1.72 ± 0.22	1.76 ± 0.31	1.83 ± 0.18	2.01 ± 0.37	2.19 ± 0.32
Cell roundness	0.58 ± 0.08	0.57 ± 0.10	0.55 ± 0.06	0.50 ± 0.11	0.46 ± 0.07

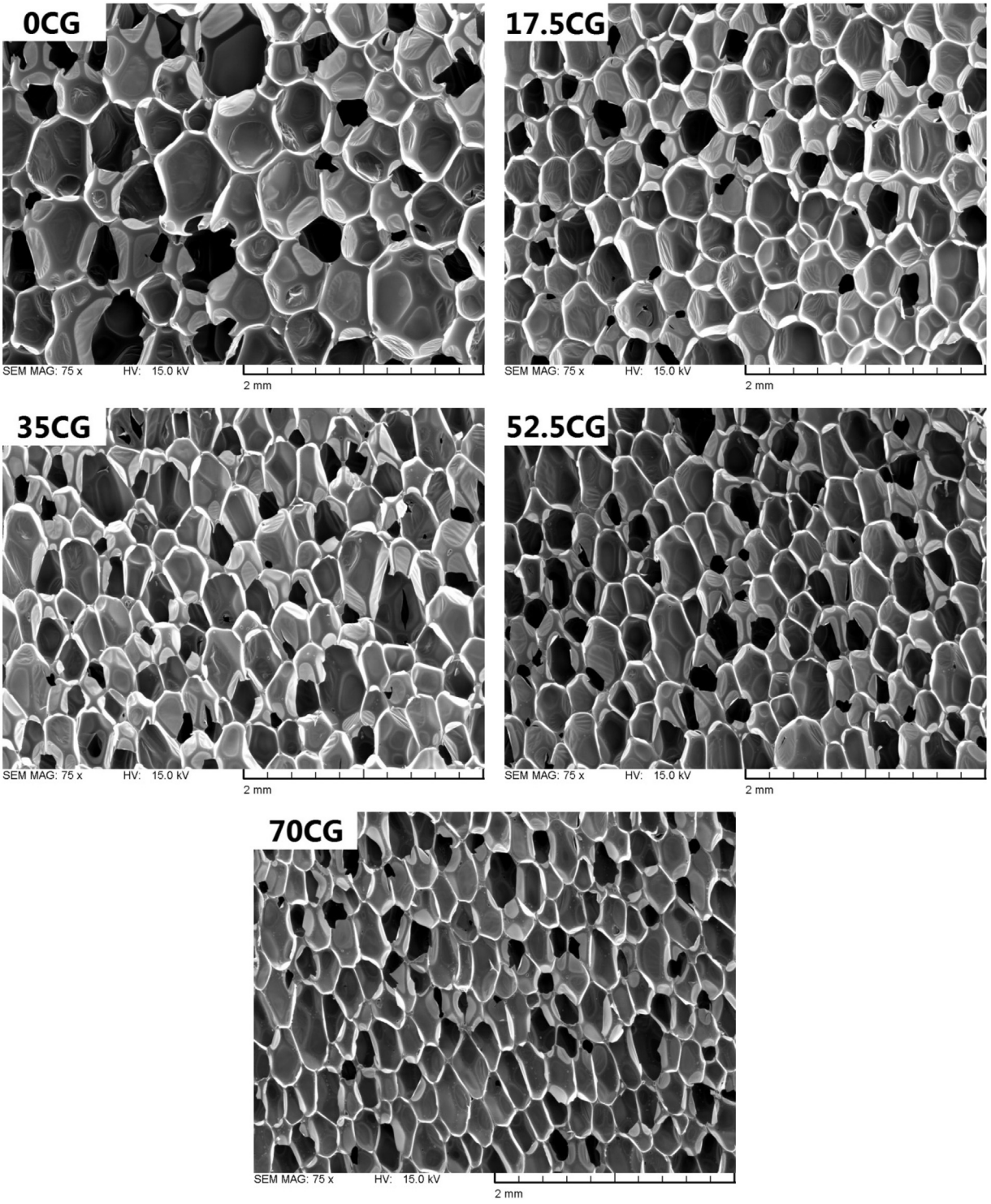

Fig. 7. SEM micrographs of rigid polyurethane foams.

aspect ratio (AR) and roundness (R)) were calculated using computer software from SEM images of prepared foams. In order to calculate shape descriptors software fitted ellipses into foams' cells and used the following Formulas ((2) and (3)):

$$AR = \frac{L_l}{L_s} \tag{2}$$

$$R = 4 \cdot \frac{A}{\pi \cdot L_l^2} \tag{3}$$

where: L_l and L_s mean the length of longer and shorter axis of fitted ellipse and A is the area of ellipse.

For perfect circle, values of AR and R are equal to one. It can be seen that increasing biopolyol content in polyol mixture resulted in elongation of cells in the foaming direction. Such phenomenon might be related to the higher amount of heat generated during foaming and faster evaporation of hydrofluorocarbon foaming agent. Anisotropy of the structure had also noticeable impact on the mechanical properties of obtained rigid PU-PIR foams, which can be seen further.

Thermal conductivity is a very important parameter of rigid PU-PIR foams, which has significant impact on their potential applicability, since they are very often used as thermal insulation materials. Insulating properties of foam, expressed as thermal conductivity coefficient (λ) are strictly related to the morphology and density of material. Value of λ coefficient of foam depends on following elements: λ_{gas}, $\lambda_{solidPU}$, $\lambda_{radiation}$ and $\lambda_{convection}$ (Szycher, 1999). Thermal conductivity coefficients of solid PU-PIR, Solkane 365/227 blend used as foaming agent, CO_2 generated during chemical foaming and air replacing foaming agents as foam is aging are 220.0, 10.6, 15.3 and 24.9 mW/m K, respectively (Randall and Lee, 2002). Apparent density of the material has a great influence on the share of these elements in total thermal conductivity coefficient of material. In case of higher density, λ of the foam will depend more on the $\lambda_{solidPU}$ than on the λ_{gas}. Therefore, foams having relatively low apparent density are preferred for thermal insulation materials. Other important factors are size and type of cells present in the structure of foam. Value of $\lambda_{radiation}$ is strictly correlated with the cell size according to Formulas (Glicksman, 1994) ((4) and (5)):

$$\lambda_{radiation} = \frac{16\sigma T^3}{3K} \tag{4}$$

where:

$$K = 4.1 \cdot \frac{\sqrt{f_s \frac{\rho_f}{\rho_p}}}{d} \tag{5}$$

where: σ is Stefan-Boltzmann constant and equals $5.67 \cdot 10^{-8}$ W/m^2 K^4; T is temperature; K means Rosseland mean extinction coefficient; f_s is fraction of polymer in struts; ρ_f and ρ_p density of foam and polymer, respectively; and d is cell diameter.

Basing of presented equations it is clear that the increase of cell size causes simultaneous increase of $\lambda_{radiation}$ and therefore increase of total λ value of foam. It has been proved that the increase of average cell diameter from 0.25 to 0.60 mm caused the increase of thermal conductivity coefficient by almost 50% (Randall and Lee, 2002). Moreover, foams with open-cell structure show higher $\lambda_{convection}$ comparing to closed-cell structure, in latter case conductivity through convection can be omitted (Bogdan et al., 2005).

In Fig. 8 there is shown the effect of prepared biopolyol content in polyol mixture on the closed cell content and thermal conductivity coefficients of resulting rigid PU-PIR foams. Closed cell content of reference foam was 94%, while substitution of up to 52.5 wt.% of petrochemical polyol with biopolyol CG increased value of this parameter over 95% (95.3, 95.7 and 95.1 for 17.5, 35.0 and 52.5 wt.% of CG, respectively). Complete substitution of Lupranol 3300 with

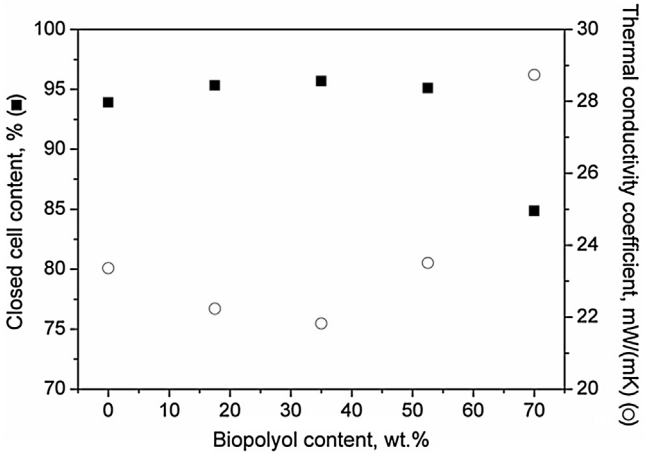

Fig. 8. Values of closed cell content and thermal conductivity coefficients of rigid PU-PIR foams.

CG resulted in deterioration of foam's cellular structure and resulting foam contained only 85% of closed cells. Similar results related to the application of crude glycerol-based polyol were obtained in other work (Piszczyk et al., 2014b). Value of λ for reference foam was 23.4 mW/m K. Modification of foam system with 17.5 and 35.0 wt.% of biopolyol caused reduction of this parameter to 22.2 and 21.8 mW/m K, respectively, which is comparable with the thermal conductivity coefficient of commercially available products. Such enhancement of thermal insulation properties can be associated with high content of closed cells and decrease of cell size comparing to unmodified foam. Incorporation of 52.5 wt.% of CG resulted in slight increase of λ value to 23.5 mW/m K, but further increase of biopolyol content increased λ value to 28.7 mW/m K, which correlates with the deterioration of cellular structure of rigid foam. In case of foam containing 70 wt.% of biopolyol in polyol mixture, the increase of thermal conductivity coefficient is strictly related to the changing share of Solkane 365/227 in hydrofluorocarbon/air system filing the pores of foam. As mentioned before λ value of used physical foaming agent is almost 2.5 times lower than λ value of air.

Compressive performance of foamed materials is strictly correlated with their apparent density, since during compression the stiffness of the material arises from buckling of cell walls and higher density is obviously related to the more compact cellular structure (Mosiewicki et al., 2009). In Fig. 9 there are presented values of compressive strength and modulus of investigated rigid PU-PIR foams. It can be seen that incorporation of prepared biopolyol resulted in the enhancement of foams' mechanical performance, despite of the slight decrease of apparent density (Table 4). Moreover, presented data clearly indicates that morphology of the foam has a crucial influence on its mechanical strength. Anisotropy of the structure, observed on SEM images, resulted in the differences in compressive strength and modulus along the directions parallel and perpendicular to the foam rise. Such phenomenon was also observed in other works (Kurańska et al., 2015; Modesti and Lorenzetti, 2003). Mechanical anisotropy was increasing with biopolyol content, however in case of 70CG foam, values of compressive strength along both axes are quite close, despite the high value of cell aspect ratio, which can be related to the unfavorable changes in cellular structure, e.g. lower closed cell content.

The plot of loss tangent (tan δ) as function of temperature is presented in Fig. 10. It can be seen, that the substitution of petrochemical polyol with biopolyol shifts the temperature position of maximum value of tan δ peak towards higher temperature. Position of these peaks can be used to determine the glass transition temperature (T_g) of material. According to presented data T_g of

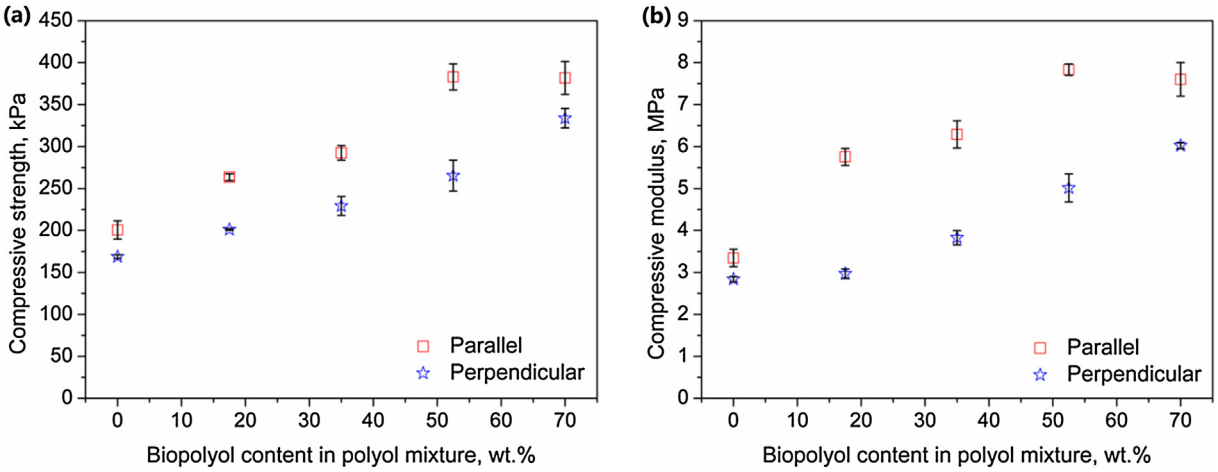

Fig. 9. Values of compressive strength (a) and compressive modulus (b) of prepared rigid PU-PIR foams.

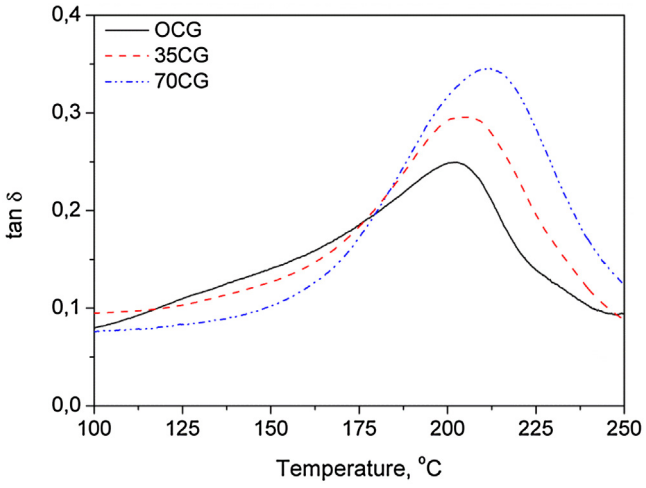

Fig. 10. Plot of loss tangent of rigid PU-PIR foams as a function of temperature.

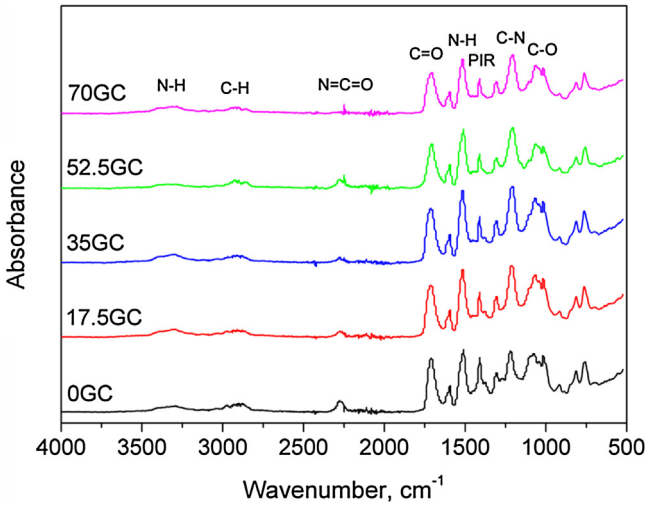

Fig. 11. FTIR spectra of prepared rigid polyurethane foams.

sample 0CG was 202.3 °C, while incorporation of 35 and 70 wt.% of prepared biopolyol increased T_g to 205.4 and 211.2 °C, respectively. Moreover, increasing content of crude glycerol based polyol in PU-PIR foam shows noticeable impact on the peak magnitude. The magnitude of the tan δ peak is strictly correlated with the nature of polymer material and the ability of the material to dissipate energy by internal friction and molecular motions. High value of loss tangent is characteristic for materials with a high, non-elastic strain component, while a low value indicates one that is more elastic (Bindu and Thomas, 2013). As it can be seen in the presented plot, tan δ peak is noticeably increasing with the rising share of biopolyol in polyol mixture, which can be associated with the enhanced mobility of polymer chains in foams' structure. Values of tan δ can be associated with the results of compression tests, foams with higher content of biopolyol can withstand higher stress, due to the enhanced ability to energy dissipation by molecular motions. It was also observed that the modifications of reference foam with bio-based polyol resulted in the sharpening of the peak, indicating sharper distribution of relaxation times in 70CG sample comparing to those with lower content of biopolyol (Abdalla et al., 2007).

The FTIR spectra of the produced foams are presented in Fig. 11. A signal characteristic for stretching vibrations of N—H groups (in urethane linkages) was observed in the range 3290–3320 cm^{-1}. Bands attributed to the bending vibrations of these groups were observed at 1510–1520 cm^{-1} (Sormana and Meredith, 2004). The absorption maxima at 1705–1715 cm^{-1} were corresponding to the stretching vibrations of C═O bonds. Signals at 1200–1215 cm^{-1} can be associated with stretching vibrations of C—N bonds in urethane linkages (Fournier and Du Prez, 2008). The aforementioned absorption bands confirm the presence of urethane bonds in the investigated material. The signals at 2860–2870 and 2960–2975 cm^{-1} were attributable to the symmetric and asymmetric stretching vibrations of C—H bonds in CH_2 groups present in aliphatic chains and CH_3 end groups. Low intensity peaks at 2260–2280 cm^{-1} resulted from the presence of unreacted —N═C═O groups, due to the excess of isocyanate used during manufacturing of foams (Jiao et al., 2013). Signals at 1410–1415 cm^{-1} were assigned to the presence of isocyanurate rings, products of the isocyanate trimerization (Samborska-Skowron and Balas, 2003). Multiplet bands in the range of 1000–1090 cm^{-1} were associated with the presence of δ bonds between carbon and oxygen atoms (in the case of ether bonds), which is related to the structure of used polyols (Pretsch et al., 2009).

The mechanism of the thermal degradation of PU is often described as very complex, due to the complex structure of PU. At the beginning, evaporation or thermal decomposition of easily volatilized additives may occur. The first stage of actual PU degradation (around 300 °C) involves dissociation of biuret, allophanate and urethane bonds, followed by thermal decomposition leading to the formation of amines, small transition components and carbon

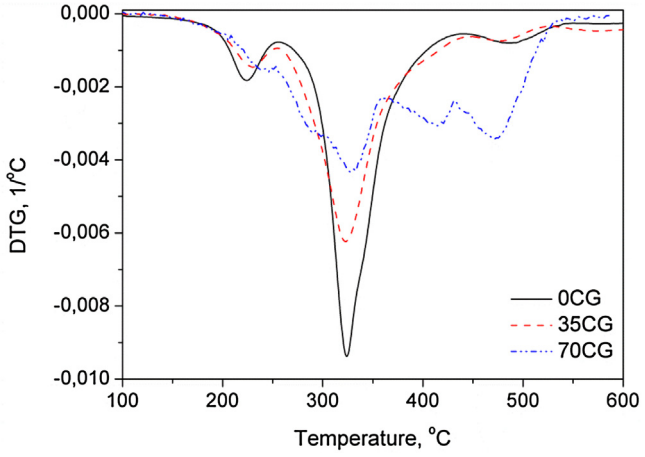

Fig. 12. Differential thermogravimetric curves of rigid PU-PIR foams.

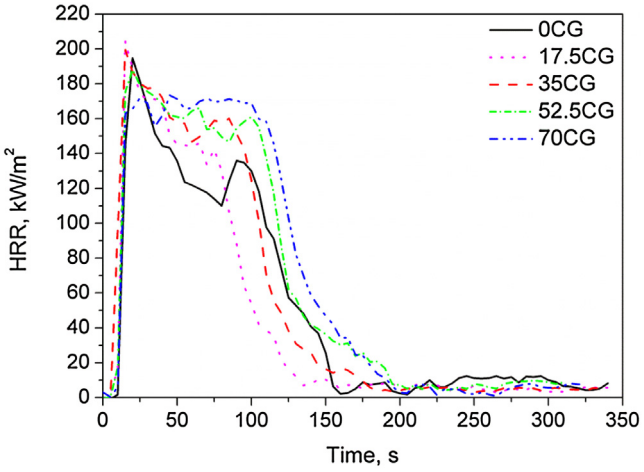

Fig. 13. Plots of HRR for prepared PU-PIR foams.

dioxide (Somania et al., 2003; Tanaka et al., 2008). Later stages are related to the decomposition of long polyether or polyester chains, depending of the structure of used polyol, and are relatively slower than the first step (Cervantes-Uc et al., 2009; Pawlik and Prociak, 2012). Obviously, the rate of degradation in all steps depends very strongly on the chemical structure of polymer matrix.

Performed thermogravimetric analysis revealed that there are no significant differences in thermal stability of prepared PU-PIR foams. Temperature related to the onset of degradation, associated with the evaporation of easily volatilized products (Wrześniewiska-Tosik et al., 2014) was quite similar for all samples. No deterioration of thermal stability, often related to the incorporation of bio-based materials into polyurethane foams, was observed (Septevani et al., 2015).

In Table 5 there are presented values of $T_{max\,1}$, $T_{max\,2}$, $T_{max\,3}$ and $T_{max\,4}$, which correspond to the temperature positions of peaks on differential thermogravimetric curves. These are temperatures, when thermal degradation occurs in the most rapid manner. Moreover, DTG curves of samples 0CG, 35CG, 70CG are presented in Fig. 12 in order to show the changes in thermal degradation pathway. Peak $T_{max\,1}$ can be associated with the decomposition of TCPP (decomposes at 244 °C) used during synthesis, value of mass loss corresponds with the amount of TCPP added to polyol mixture. It can be seen that the increase of CG biopolyol in PU-PIR foam caused shift of peak $T_{max\,2}$, related to thermal degradation of biuret, allophanate and urethane bonds, towards higher temperatures. Therefore, thermal stability of rigid segments was enhanced with the increasing content of CG biopolyol. Separate peak $T_{max\,3}$, associated with decomposition of soft segments was observed for foams 52.5CG and 70CG, while for other samples it was overlapping with the peak $T_{max\,2}$. As mentioned above, degradation of soft phase is slower than in case of rigid segments, which is confirmed by the magnitude of proper peaks. Finally, peak $T_{max\,4}$, was related to thermolysis of the organic residues from previous steps occurring above 475 °C (Zhang et al., 2013).

In order to investigate flammability of prepared rigid PU-PIR foams, they were examined using cone calorimeter. Cone calorimetry plays an important role in assessing the fire behavior of materials. It allows the determination of various parameters characterizing combustion of material, such as heat release rate (HRR), amount of released heat and smoke, yield of gases generated during combustion and others. Typically, analyzed material is subjected to heat irradiation with intensity similar to that experienced in fire situation, from 25 to 75 kW/m^2 (Berta et al., 2006). In Table 6 there are presented values of parameters characterizing combustion of prepared foams, while in Fig. 13 there are plots of HRR for investigated materials.

HRR is very important parameter characterizing combustion of materials, because it is directly related to the speed of fire spread. Obtained HRR plots are typical of thick charring materials, initial increase in HRR is observed, until efficient char layer is formed. Other peaks may arise as a result of crack formation in char layer (Schartel and Hull, 2007). It can be seen that increasing share of CG biopolyol in polyol mixture did not increase the height of peaks. According to literature data, peak HRR (pHRR) for unmodified rigid PU-PIR foams is above 300 kW/m^2 (Qian et al., 2014), however for all investigated materials it hardly exceeded 200 kW/m^2, which can be considered as advantage of prepared foams. Moreover, pHRR values are decreasing with the increasing content of crude glycerol-based polyol. The amount of heat generated at the most critical moment of combustion is reduced and char layer formation on the surface of burning foam occurs very rapidly. It can be also seen that char layer is actually acting as a protection, since increasing amount of CG biopolyol in foam results in higher value of char residue after combustion. However, applied modifications resulted in broader HRR peaks, which means that heat is released for the longer time, simultaneously increasing total heat released (THR).

Formation of toxic carbon monoxide is another important parameter of combustion. It can be seen that incorporation of CG

Table 5
Characteristics of thermal degradation in rigid polyurethane foams.

Sample	Onset of degradation, °C	Mass loss, %		T_{max1}, °C	T_{max2}, °C	T_{max3}, °C	T_{max4}, °C
		5	10				
		Temperature, °C					
0CG	200.8	228.1	276.5	223.7	324.0	–	487.5
17.5CG	200.4	227.4	274.3	225.4	324.4	–	475.1
35CG	197.4	232.4	274.8	229.8	324.9	–	478.4
52.5CG	198.5	229.7	268.4	230.1	325.7	413.6	473.4
70CG	198.3	232.4	264.5	236.2	327.2	413.8	471.3

Table 6
Parameters describing flammability of prepared rigid PU-PIR foams.

Sample	pHRR[a], kW/m^2	THR[b], MJ/m^2	TSR[c], m^2/m^2	EHC_{av}[d], MJ/kg	COY_{av}[e], kg/kg	CO_2Y_{av}[f], kg/kg	Char residue, wt.%
0CG	190.5 ± 6.1	16.5 ± 1.0	759 ± 4	17.2 ± 1.3	0.17 ± 0.01	3.0 ± 0.5	12.0 ± 2.1
17.5CG	198.1 ± 6.8	15.4 ± 0.6	774 ± 59	16.1 ± 0.6	0.20 ± 0.02	3.0 ± 0.2	14.1 ± 3.0
35CG	193.6 ± 5.3	18.9 ± 0.6	1030 ± 46	15.4 ± 0.5	0.14 ± 0.00	2.4 ± 0.1	13.5 ± 2.8
52.5CG	184.2 ± 5.4	20.2 ± 0.5	1052 ± 3	15.4 ± 0.5	0.12 ± 0.01	2.3 ± 0.1	14.7 ± 1.4
70CG	184.1 ± 9.7	21.9 ± 0.4	1176 ± 93	15.6 ± 0.1	0.11 ± 0.00	2.2 ± 0.1	14.9 ± 0.7

[a] Peak heat release rate.
[b] Total heat release.
[c] Total smoke release.
[d] Average effective heat of combustion.
[e] Average yield of carbon oxide.
[f] Average yield of carbon dioxide.

biopolyol resulted in reduced emission of this compound during burning of rigid PU-PIR foams, which can be associated with the quick formation of protective char layer (Zheng et al., 2014).

The effective heat of combustion (EHC) measured in the cone calorimeter corresponds mostly to the flame burning condition and thus to combustion of volatiles from material. It is calculated from the ratio of values of total heat evolved and mass loss within specified time. As it can be seen in Table 6, EHC_{av} is decreasing with the increasing share of CG biopolyol, which means that less heat is released from the volatile portion during solid material combustion. It can be considered as beneficial issue, since volatiles released from the burning material are transferring lower amount of heat to the surrounding and fire spread is less probable.

Generally it can be seen that the incorporation of CG bio-based polyol into rigid PU-PIR foams results in changes in combustion mechanism and pathway. More detailed analysis of this process will be further studied.

4. Conclusions

Biopolyol synthesized from two products of industrial crops' processing: crude glycerol and castor oil was applied in the production of rigid PU-PIR foams. In order to obtain bio-based polyol, crude glycerol was polymerized using residual potassium hydroxide from biodiesel production as a catalyst. Resulting polyglycerol was further condensed with castor oil in order to reduce viscosity of the product. Such biopolyol, was characterized with the hydroxyl value of 460 mg KOH/g, density of 1.18 g/cm^3 and water content of 0.207 wt.%. Basic rheological analysis of biopolyol was also performed and revealed its dilatant character. Rigid PU-PIR foams were prepared at partial substitution (0–70 wt.%) of petrochemical polyol with bio-based polyol. Formulations of foams were adjusted to provide the same apparent density of analyzed materials. Increasing content of biopolyol reduced the amount of hydrofluorocarbon foaming agent necessary to provide the same volumetric expansion of material during synthesis, which can be very beneficial from the economic and technological point of view. Incorporation of crude glycerol-based polyol into formulation of rigid foams had also beneficial influence on the structure of material. Average cell size was reduced even by 25% and closed cell content increased by almost 2%, which resulted in decrease of thermal conductivity coefficient from 23.4 to 21.8 mW/m K in case of 35 wt.% content of biopolyol in polyol mixture. Substitution of petrochemical polyol with bio-based one caused elongation of cells in foaming direction, which may be related to the increased heat generation and enhanced evaporation of physical foaming agent. Anisotropy of the structure was strictly correlated with the differences in mechanical performance parallel and perpendicularly to the foaming direction. Compressive strength of the foams increased with the rising share of biopolyol in polyol mixture, which was related to the enhanced ability to energy dissipation by molecular motions and internal frictions. As a result material was able to withstand higher stress without destruction of its structure. Regarding thermal stability, modifications with biopolyol did not have any unfavorable influence on foams performance, thermal stability of material prepared solely with petrochemical polyols was maintained even for 70 wt.% substitution with bio-based polyol. Increasing share of CG polyol resulted in changes in combustion pathway, which can be considered beneficial for the human safety, since peak heat release rate, effective heat of combustion and yield of toxic carbon monoxide were decreased.

Summarizing, this work confirms that crude glycerol, as a by-product from biodiesel production, can be successfully applied in biopolyols production, which can be a low-cost alternative for conventional, petroleum-based polyols for rigid PU-PIR foams. Such solution can be considered very beneficial from the ecological and economical point of view, due to the utilization of waste material from renewable raw materials processing. Furthermore, obtained results and present state-of-the-art indicate that further studies on that field should focus on: i) investigation of the full substitution of petrochemical polyols with those obtained from crude glycerol during production of PU-PIR foams; ii) evaluation of the impact of crude glycerol impurities on manufacturing and properties of rigid foams; iii) more detailed examination of combustion of crude glycerol-based rigid PU-PIR foams.

References

Abdalla, M., Dean, D., Adibempe, D., Nyairo, E., Robinson, P., Thompson, G., 2007. The effect of interfacial chemistry on molecular mobility and morphology of multiwalled carbon nanotubes epoxy nanocomposite. Polymer 48, 5662–5670, http://dx.doi.org/10.1016/j.polymer.2007.06.073.

Allauddin, S., Somisetti, V., Ravinder, T., Rao, B.V.S.K., Narayan, R., Raju, K.V.S.N., 2016. One-pot synthesis and physiochemical properties of high functionality soy polyols and their polyurethane-urea coatings. Ind. Crops Prod. 85, 361–371, http://dx.doi.org/10.1016/j.indcrop.2015.12.087.

Amir Uddin, M.A., Azad, A.K., 2012. Diesel engine performance study for bio-fuel: vegetable oil, a alternative source of fuel. Int. J. Energy Mach. 5, 8–17.

Andersons, J., Kirpluks, M., Stiebra, L., Cabulis, U., 2015. The effect of a circular hole on the tensile strength of neat and filled rigid PUR foams. Theor. Appl. Fract. Mech. 78, 8–14, http://dx.doi.org/10.1016/j.tafmec.2015.05.001.

Arshanitsa, A., Krumina, L., Telysheva, G., Dizhbite, T., 2016. Exploring the application potential of incompletely soluble organosolv lignin as a macromonomer for polyurethane synthesis. Ind. Crops Prod. 2016, 1–12, http://dx.doi.org/10.1016/j.indcrop.2016.07.050.

Berta, M., Lindsay, C., Pans, G., Camino, G., 2006. Effect of chemical structure on combustion and thermal behavior of polyurethane elastomer layered silicate nanocomposites. Polym. Degrad. Stab. 91, 1179–1191, http://dx.doi.org/10.1016/j.polymdegradstab.2005.05.027.

Bindu, P., Thomas, S., 2013. Viscoelastic behavior and reinforcement mechanism in rubber nanocomposites in the vicinity of spherical nanoparticles. J. Phys. Chem. B 117, 12632–12648, http://dx.doi.org/10.1021/jp4039489.

Bogdan, M., Hoerter, J., Moore, F.O., 2005. Meeting the insulation requirements of the building envelope with polyurethane and polyisocyanurate foam. J. Cell. Plast. 41, 41–56, http://dx.doi.org/10.1177/0021955X05049869.

Budarin, V.L., Clark, J.H., Lanigan, B.A., Shuttleworth, P., Macquarrie, D.J., 2010. Microwave assisted decomposition of cellulose: a new thermochemical route for biomass exploitation. Bioresour. Technol. 101, 3776–3779, http://dx.doi.org/10.1016/j.biortech.2009.12.110.

Cai, Z., Gao, J., Li, X., Xiang, B., 2007. Synthesis and characterization of symmetrical benzodifuranone compounds with femtosecond time-resolved degenerate four-wave mixing technique. Opt. Commun. 272, 503–508, http://dx.doi.org/10.1016/j.optcom.2006.11.056.
Casiello, M., Monopoli, A., Cotugno, P., Milella, A., Dell'Anna, M.M., Ciminale, F., Nacci, A., 2014. Copper(II) chloride-catalyzed oxidative carbonylation of glycerol to glycerol carbonate. J. Mol. Catal. A-Chem. 381, 99–106, http://dx.doi.org/10.1016/j.molcata.2013.10.006.
Cassel, S., Debaig, C., Benvegnu, T., Chaimbault, P., Lafosse, M., Plusquellec, D., Rollin, P., 2001. Original synthesis of linear, branched and cyclic oligoglycerol standards. Eur. J. Org. Chem. 2001, 875–896, http://dx.doi.org/10.1002/1099-0690(200103)2001:5<875:AID-EJOC875>3.0.CO;2-R.
Cervantes-Uc, J.M., Moo Espinosa, J.I., Cauich-Rodriguez, J.V., Avila-Ortega, A., Vazquez-Torres, H., Marcos-Fernandez, A., San Roman, J., 2009. TGA/FTIR studies of segmented aliphatic polyurethanes and their nanocomposites prepared with commercial. Polym. Degrad. Stab. 94, 1666–1677, http://dx.doi.org/10.1016/j.polymdegradstab.2009.06.022.
Cheng, D., Wang, L., Shahbazi, A., Xiu, S., Zhang, B., 2014. Characterization of the physical and chemical properties of the distillate fractions of crude bio-oil produced by the glycerol-assisted liquefaction of swine manure. Fuel 130, 251–256, http://dx.doi.org/10.1016/j.fuel.2014.04.022.
Chhabra, R.P., 2010. Non-Newtionian fluids: an introduction. In: Deshpande, A.P., Krishan, J.M., Kumar, S. (Eds.), Rheology of Complex Fluids. Springer-Verlag, New York, pp. 3–34, http://dx.doi.org/10.1007/978-1-4419-6494-6_1.
Choi, W.J., 2008. Glycerol-based biorefinery for fuels and chemicals. Recent Pat. Biotechnol. 2, 173–180, http://dx.doi.org/10.2174/187220808786241006.
Clacens, J.M., Pouilloux, Y., Barrault, J., 2000. Synthesis and modification of basic mesoporous materials for the selective etherification of glycerol. Stud. Surf. Sci. Catal. 143, 687–695, http://dx.doi.org/10.1016/S0167-2991(00)80711-9.
Deng, S., Ting, Y.P., 2005. Characterization of PEI-modified biomass and biosorption of Cu (II), Pb (II) and Ni (II). Water Res. 39, 2167–2177.
Dziubiński, M., Kiljański, T., Sęk, J., 2009. Podstawy reologii i reometrii płynów. Lodz University of Technology Publisher, Lodz, Poland.
Ezhova, N.N., Korosteleva, I.G., Kolesnichenko, N.V., Kuzmin, A.E., Khadzhiev, S.N., Vasileva, M.A., Voronina, Z.D., 2012. Glycerol carboxylation to glycerol carbonate in the presence of rhodium complexes with phosphine ligands. Petrol. Chem. 52, 91–96, http://dx.doi.org/10.1134/S0965544112020041.
Fournier, D., Du Prez, F., 2008. Click chemistry as a promising tool for side-chain functionalization of polyurethanes. Macromolecules 41, 4622–4630, http://dx.doi.org/10.1021/ma800189z.
Glicksman, L.R., 1994. Heat transfer in foams. In: Hylyard, N.C., Cunningham, A. (Eds.), Low Density Cellular Plastics. Kluwer Academic Publishers, Dordrecht, pp. 115–116, http://dx.doi.org/10.1007/978-94-011-1256-7.
Hoekman, S.K., Broch, A., Robbins, C., Ceniceros, E., Natarajan, M., 2012. Review of biodiesel composition, properties, and specifications. Renew. Sustain. Energy Rev. 16, 143–169, http://dx.doi.org/10.1016/j.rser.2011.07.143.
Hu, S., Li, Y., 2014. Polyols and polyurethane foams from base-catalyzed liquefaction of lignocellulosic biomass by crude glycerol: effects of crude glycerol impurities. Ind. Crops Prod. 57, 188–194, http://dx.doi.org/10.1016/j.indcrop.2014.03.032.
Hu, S., Wan, C., Li, Y., 2012. Production and characterization of biopolyols and polyurethane foams from crude glycerol based liquefaction of soybean straw. Bioresour. Technol. 103, 227–233, http://dx.doi.org/10.1016/j.biortech.2011.09.125.
Ionescu, M., Petrovic, Z.S., 2010. High functionality polyether polyols based on polyglycerol. J. Cell. Plast. 46, 223–237, http://dx.doi.org/10.1177/0021955X09355887.
Jagadeeswaraiah, K., Kumar, C.R., Sai Prasad, P.S., Loridant, S., Lingaiah, N., 2014. Synthesis of glycerol carbonate from glycerol and urea over tin-tungsten mixed oxide catalysts. Appl. Catal. A-Gen. 469, 165–172, http://dx.doi.org/10.1016/j.apcata.2013.09.041.
Jiao, L., Xiao, H., Wang, Q., Sun, J., 2013. Thermal degradation characteristics of rigid polyurethane foam and the volatile products analysis with TG-FTIR-MS. Polym. Degrad. Stab. 98, 2687–2696, http://dx.doi.org/10.1016/j.polymdegradstab.2013.09.032.
Kainthan, R.K., Muliawan, E.B., Hatzikiriakos, S.G., Brooks, D.E., 2006. Synthesis, characterization, and viscoelastic properties of high molecular weight hyperbranched polyglycerols. Macromolecules 39, 7708–7717, http://dx.doi.org/10.1021/ma0613483.
Kairyte, A., Vejelis, S., 2015. Evaluation of forming mixture composition impact on properties of water blown rigid polyurethane (PUR) foam from rapeseed oil polyol. Ind. Crops Prod. 6, 210–215, http://dx.doi.org/10.1016/j.indcrop.2014.12.032.
Ćirpluks, M., Cabilis, U., Zeltins, V., Stiebra, L., Avots, A., 2014. Rigid polyurethane foam thermal insulation protected with mineral intumescent mat. Autex Res. J. 14, 259–269, http://dx.doi.org/10.2478/aut-2014-0026.
Člepáčová, K., Mravec, D., Bajus, M., 2005. tert-Butylation of glycerol catalyzed by ion- exchange resins. Appl. Catal. A-Gen. 294, 141–147, http://dx.doi.org/10.1016/j.apcata.2005.06.027.
Ćurańska, M., Prociak, A., 2016. The influence of rapeseed oil-based polyols on the foaming proces of rigid polyurethane foams. Ind. Crops Prod. 89, 182–187, http://dx.doi.org/10.1016/j.indcrop.2016.05.016.
Ćurańska, M., Prociak, A., Kirpluks, M., Cabulis, U., 2015. Polyurethane–polyisocyanurate foams modified with hydroxyl derivatives of rapeseed oil. Ind. Crops Prod. 74, 849–857, http://dx.doi.org/10.1016/j.indcrop.2015.06.006.
Kurańska, M., Cabulis, U., Auguścik, M., Prociak, A., Ryszkowska, J., Kirpluks, M., 2016. Bio-based polyurethane-polyisocyanurate composites with an intumescent flame retardant. Polym. Degrad. Stab. 127, 11–19, http://dx.doi.org/10.1016/j.polymdegradstab.2016.02.005.
Li, C., Luo, X., Li, T., Tong, X., Li, Y., 2014. Polyurethane foams based on crude glycerol-derived biopolyols: one-pot preparation of biopolyols with branched fatty acid ester chains and its effects on foam formation and properties. Polymer 55, 6529–6538, http://dx.doi.org/10.1016/j.polymer.2014.10.043.
Luo, X., Hu, S., Zhang, X., Li, Y., 2013. Thermochemical conversion of crude glycerol to biopolyols for the production of polyurethane foams. Bioresour. Technol. 139, 323–329, http://dx.doi.org/10.1016/j.biortech.2013.04.011.
Melero, J.A., Vicente, G., Paniagua, M., Morales, G., Muñoz, P., 2012. Etherification of biodiesel-derived glycerol with ethanol for fuel formulation over sulfonic modified catalysts. Bioresour. Technol. 103, 142–151, http://dx.doi.org/10.1016/j.biortech.2011.09.105.
Miyata, A., Tsutsui, T., Konga, N., Matsumoto, S., Ohkubo, K., 2012. Polyether polyol, hard polyurethane foam and their production methods. Patent EP2080778.
Modesti, M., Lorenzetti, A., 2003. Improvement on fire behaviour of water blown PIR–PUR foams: use of an halogen-free flame retardant. Eur. Polym. J. 39, 263–268, http://dx.doi.org/10.1016/s0014-3057(02)00198-2.
Mosiewicki, M.A., Dell'Arciprete, G.A., Aranguren, M.I., Marcovich, N.E., 2009. Polyurethane foams obtained from castor oil-based polyol and filled with wood flour. J. Compos. Mater. 43, 3057–3072, http://dx.doi.org/10.1177/0021998309345342.
Nguyen, N., Demirel, Y., 2013. Economic analysis of biodiesel and glycerol carbonate production plant by glycerolysis. J. Sustain. Bioenergy Syst. 3, 209–216, http://dx.doi.org/10.4236/jsbs.2013.33029.
Nik Siti, M.N.M.D., Idris, Z., Shoot, K.Y., Hassan, H.A., 2013. Preparation of polyglycerol from palm-biodiesel crude glycerin. J. Oil Palm Res. 25, 289–297.
Pawlik, H., Prociak, A., 2012. Influence of palm oil-based polyol on the properties of flexible polyurethane foams. J. Polym. Environ. 20, 438–445, http://dx.doi.org/10.1007/s10924-011-0393-2.
Petrov, K., Petrova, P., 2010. Enhanced production of 2,3-butanediol from glycerol by forced pH fluctuations. Appl. Microbiol. Biotechnol. 87, 943–949, http://dx.doi.org/10.1007/s00253-010-2545-z.
Piszczyk Ł., Danowska M., Haponiuk J., Strankowski M., 2014. Sposób wytwarzania ekologicznych polioli z odpadu po transestryfikacji olejów roślinnych oraz sposób wytwarzania sztywnych pianek poliuretanowych. Patent application P.408610.
Piszczyk, Ł., Strankowski, M., Danowska, M., Hejna, A., Haponiuk, J.T., 2014b. Rigid polyurethane foams from a polyglycerol-based polyol. Eur. Polym. J. 57, 143–150, http://dx.doi.org/10.1016/j.eurpolymj.2014.05.012.
Pretsch, T., Jakob, I., Müller, W., 2009. Hydrolytic degradation and functional stability of a segmented shape memory poly(ester urethane). Polym. Degrad. Stab. 94, 61–73, http://dx.doi.org/10.1016/j.polymdegradstab.2008.10.012.
Puri, M., Abraham, R.E., Barrow, C.J., 2012. Biofuel production: prospects, challenges and feedstock in Australia. Renew. Sustain. Energy Rev. 16, 6022–6031, http://dx.doi.org/10.1016/j.rser.2012.06.025.
Qian, L., Feng, F., Tang, S., 2014. Bi-phase flame-retardant effect of hexa-phenoxy-cyclotriphosphazene on rigid polyurethane foams containing expandable graphite. Polymer 55, 95–101, http://dx.doi.org/10.1016/j.polymer.2013.12.015.
Ragauskas, A.J., Williams, C.K., Davison, B.H., Britovsek, G., Cairney, J., Eckert, C.A., Frederick Jr., W.J., Hallett, J.P., Leak, D.J., Liotta, C.L., Mielenz, J.R., Murphy, R., Templer, R., Tschaplinski, T., 2006. The path forward for biofuels and biomaterials. Science 311, 484–489, http://dx.doi.org/10.1126/science.1114736.
Randall, D., Lee, S., 2002. The Polyurethanes Book. John Wiley & Sons, Ltd, New York.
Salehpour, S., Dubé, M.A., 2011. Towards the sustainable production of higher-molecular-weight polyglycerol. Macromol. Chem. Phys. 212, 1284–1293, http://dx.doi.org/10.1002/macp.201100064.
Salehpour, S., Dubé, M.A., 2012. Reaction monitoring of glycerol step-growth polymerization using ATR-FTIR spectroscopy. Macromol. React. Eng. 6, 85–92, http://dx.doi.org/10.1002/mren.201100071.
Samborska-Skowron, R., Balas, A., 2003. Jakościowa identyfikacja pierścieni izocyjanurowych w elastomerach uretanowo-izocyjanurowych i w ich hydrolizatach. Polimery 48, 371–374.
Schartel, B., Hull, T.R., 2007. Development of fire-retarded materials—interpretation of cone calorimeter data. Fire Mater. 31, 327–354, http://dx.doi.org/10.1002/fam.949.
Scholz, V., da Silva, J.N., 2008. Prospects and risks of the use of castor oil as a fuel. Biomass Bioenergy 32, 95–100, http://dx.doi.org/10.1016/j.biombioe.2007.08.004.
Septevani, A.A., Evans, D.A.C., Chaleat, C., Martin, D.J., Annamalai, P.K., 2015. A systematic study substituting polyether polyol with palm kernel oil based polyester polyol in rigid polyurethane foam. Ind. Crops Prod. 66, 16–26, http://dx.doi.org/10.1016/j.indcrop.2014.11.053.
Singh, R.P., Heldman, D.R., 2013. Introduction to Food Engineering, 5th ed. Elsevier, Amsterdam.
Somania, K.P., Kansaraa, S.S., Patelb, N.K., Rakshit, A.K., 2003. Castor oil based polyurethane adhesives for wood-to-wood bonding. Int. J. Adhes. Adhes. 23, 269–275, http://dx.doi.org/10.1016/S0143-7496(03)00044-7.
Sormana, J.L., Meredith, J.C., 2004. High-throughput discovery of structure-mechanical property relationships for segmented

poly(urethane-urea)s. Macromolecules 37, 2186–2195, http://dx.doi.org/10.1021/ma035385v.
Szycher, M., 1999. Szycher's Handbook of Polyurethanes, first ed. CRC Press, Boca Raton, Florida.
Szymanowska-Powałowska, D., 2014. 1,3-Propanediol production from crude glycerol by Clostridium butyricum DSP1 in repeated batch. Electron. J. Biotechnol. 17, 322–328, http://dx.doi.org/10.1016/j.ejbt.2014.10.001.
Tanaka, R., Hirose, S., Hatakeyama, H., 2008. Preparation and characterization of polyurethane foams using a palm oil-based polyol. Bioresour. Technol. 99, 3810–3816, http://dx.doi.org/10.1016/j.biortech.2007.07.007.
Thompson, J.C., He, B.B., 2006. Characterization of crude glycerol from biodiesel production from multiple feedstocks. Appl. Eng. Agric. 22, 261–265, http://dx.doi.org/10.13031/2013.20272.
Tong, X., Luo, X., Li, Y., 2015. Development of blend films from soy meal protein and crude glycerol-based waterborne polyurethane. Ind. Crops Prod. 67, 11–17, http://dx.doi.org/10.1016/j.indcrop.2014.12.063.
Wirpsza, Z., Banasiak, S., 2012. Sposób wytwarzania oligoeteroli. Patent PL 210779.
Wrześniewiska-Tosik, K., Zajchowski, S., Bryśkiewicz, A., Ryszkowska, J., 2014. Feathers as a flame-retardant in elastic polyurethane foam. Fibres Text. East. Eur. 22, 119–128.
Yazdani, S.S., Gonzalez, R., 2007. Anaerobic fermentation of glycerol: a path to economic viability for the biofuels industry. Curr. Opin. Biotechnol. 18, 213–219, http://dx.doi.org/10.1016/j.copbio.2007.05.002.
Zhang, L., Zhang, M., Zhou, Y., Hu, L., 2013. The study of mechanical behavior and flame retardancy of castor oil phosphate-based rigid polyurethane foam composites containing expanded graphite and triethyl phosphate. Polym. Degrad. Stab. 98, 2784–2794, http://dx.doi.org/10.1016/j.polymdegradstab.2013.10.015.
Zhang, L., Zhang, M., Hu, L., Zhou, Y., 2014. Synthesis of right polyurethane foams with castor oil-based flame retardant polyols. Ind. Crops Prod. 52, 380–388, http://dx.doi.org/10.1016/j.indcrop.2013.10.043.
Zheng, X., Wang, G., Xu, W., 2014. Roles of organically-modified montmorilloniteand phosphorous flame retardant during the combustion of rigid polyurethanefoam. Polym. Degrad. Stab. 101, 32–39, http://dx.doi.org/10.1016/j.polymdegradstab.2014.01.015.
Zieleniewska, M., Leszczyński, M.K., Kurańska, M., Prociak, A., Szczepkowski, L., Krzyżowska, M., Ryszkowska, J., 2015. Preparation and characterisation of rigid polyurethane foams using a rapeseed oil-based polyol. Ind. Crops Prod. 74, 887–897, http://dx.doi.org/10.1016/j.indcrop.2015.05.081.